Optical antennas integrated with concentric ring gratings: electric field enhancement and directional radiation

Dongxing Wang,[1] Tian Yang,[1,2]* and Kenneth B. Crozier[1]

[1] *School of Engineering and Applied Sciences, Harvard University, Cambridge, Massachusetts 02138, USA*
[2] *University of Michigan – Shanghai Jiao Tong University Joint Institute, Shanghai 200240, China*
tianyang@sjtu.edu.cn

Abstract: We describe a means for improving the coupling of illumination to, and the collection of scattered radiation from, an optical antenna. This is achieved by integrating optical antennas with concentric ring gratings. Electromagnetic simulations demonstrate that the ring grating improves the coupling to the antenna, even if the incident illumination is focused by an aplanatic lens such as a microscope objective. Dipole radiation from the center of the structure is well collimated. Various aspects of field enhancement and dipole radiation behavior are analyzed. We propose this device for Raman scattering enhancement.

OCIS codes: (240.6680) Surface plasmons; (240.6695) Surface-enhanced Raman scattering.

References and links

1. D. A. Long, "Raman Spectroscopy," McGraw-Hill, New York, 1977.
2. K. B. Crozier, A. Sundaramurthy, G. S. Kino, and C. F. Quate, "Optical antennas: resonators for local field enhancement," J. Appl. Phys. **94**(7), 4632 (2003).
3. E. Cubukcu, E. A. Kort, K. B. Crozier, and F. Capasso, "Plasmonic laser antenna," Appl. Phys. Lett. **89**(9), 093120 (2006).
4. N. Yu, E. Cubukcu, L. Diehl, M. A. Belkin, K. B. Crozier, F. Capasso, D. Bour, S. Corzine, and G. Höfler, "Plasmonic quantum cascade laser antenna," Appl. Phys. Lett. **91**(17), 173113 (2007).
5. P. J. Schuck, D. P. Fromm, A. Sundaramurthy, G. S. Kino, and W. E. Moerner, "Improving the mismatch between light and nanoscale objects with gold bowtie nanoantennas," Phys. Rev. Lett. **94**(1), 017402 (2005).
6. H. J. Lezec, A. Degiron, E. Devaux, R. A. Linke, L. Martín-Moreno, F. J. García-Vidal, and T. W. Ebbesen, "Beaming light from a subwavelength aperture," Science **297**(5582), 820–822 (2002).
7. L. Martín-Moreno, F. J. García-Vidal, H. J. Lezec, A. Degiron, and T. W. Ebbesen, "Theory of highly directional emission from a single subwavelength aperture surrounded by surface corrugations," Phys. Rev. Lett. **90**(16), 167401 (2003).
8. M. Beruete, I. Campillo, J. S. Dolado, J. E. Rodríguez-Seco, E. Perea, F. Falcone, and M. Sorolla, ""Very low-profile "Bull's Eye" feeder antenna," IEEE Antennas Wirel. Propag. Lett. **4**(1), 365–368 (2005).
9. K. Ishihara, T. Ikari, H. Minamide, J. Shikata, K. Ohashi, H. Yokoyama, and H. Ito, "Terahertz near-field imaging using enhanced transmission through a single subwavelength aperture," Jpn. J. Appl. Phys. **44**(29), L929–L931 (2005).
10. K. Ishihara, K. Ohashi, T. Ikari, H. Minamide, H. Yokoyama, J. Shikata, and H. Ito, "Terahertz-wave near-field imaging with subwavelength resolution using surface-wave-assisted bow-tie aperture," Appl. Phys. Lett. **89**(20), 201120 (2006).
11. Q. Min, M. J. L. Santos, E. M. Girotto, A. G. Brolo, and R. Gordon, "Localized Raman enhancement from a double-hole nanostructure in a metal film," J. Phys. Chem. Lett. C **112**(39), 15098–15101 (2008).
12. A. D. Rakic, A. B. Djurisic, J. M. Elazar, and M. L. Majewski, "Optical properties of metallic films for vertical-cavity optoelectronic devices," Appl. Opt. **37**(22), 5271–5283 (1998).
13. W. L. Barnes, A. Dereux, and T. W. Ebbesen, "Surface plasmon subwavelength optics," Nature **424**(6950), 824–830 (2003).
14. D. Wang, T. Yang, and K. B. Crozier, "Charge and current reservoirs for electric and magnetic field enhancement," Opt. Express **18**(10), 10388–10394 (2010).
15. K. Sendur, W. Challener, and O. Mryasov, "Interaction of spherical nanoparticles with a highly focused beam of light," Opt. Express **16**(5), 2874–2886 (2008).
16. K. Sendur, "An integral equation based numerical solution for nanoparticles illuminated with collimated and focused light," Opt. Express **17**(9), 7419–7430 (2009).

#137744 - $15.00 USD Received 4 Nov 2010; revised 17 Dec 2010; accepted 25 Dec 2010; published 20 Jan 2011

17. K. Sendur, and A. Sahinöz, "Interaction of radially polarized focused light with a prolate spheroidal nanoparticle," Opt. Express **17**(13), 10910–10925 (2009).
18. E. M. Purcell, "Spontaneous emission probabilities at radio frequencies," Phys. Rev. **69**, 681 (1946).
19. E. C. Le Ru, and P. G. Ethchegoin, "Rigorous justification of the $|E|^4$ enhancement factor in surface enhanced Raman spectroscopy," Chem. Phys. Lett. **423**, 63 (2006).
20. B. Richards and E. Wolf, "Electromagnetic diffraction in optical systems. II. Structure of the image field in an aplanatic system," Proc. Roy. Soc. A **253** 358 (1959). [See also L. Novotny and B. Hecht, "Principles of nano-optics," Cambridge, (2006)].
21. E. Bailo, and V. Deckert, "Tip-enhanced Raman scattering," Chem. Soc. Rev. **37**(5), 921–930 (2008).
22. Y. Gorodetski, A. Niv, V. Kleiner, and E. Hasman, "Observation of the spin-based plasmonic effect in nanoscale structures," Phys. Rev. Lett. **101**(4), 043903 (2008).

1. Introduction

Highly localized and enhanced electromagnetic fields are desirable for surface enhanced Raman scattering (SERS) [1]. One means for achieving this in a reproducible manner is using optical antennas [2–5]. However, optical antennas are usually much smaller than the focal spots of microscope objectives, especially those with low to moderate numerical apertures (NAs), leaving much of the illumination power not focused onto the optical antenna. We propose a structure, consisting of an optical antenna integrated with a concentric ring grating, which provides a highly enhanced field. The ring grating not only concentrates the illumination at its center, but also collimates the radiation of a dipole located there [6–8]. Ring gratings have been studied for beam shaping [7,8], near field imaging [9,10], and localized Raman enhancement [11]. In this paper, we conduct a comprehensive study of the field enhancement and dipole radiation properties of the antenna-integrated-with-ring-grating structure, including the effects of the NA of the lens used to focus light onto, and collect light from, the structure. We consider its application in enhanced Raman scattering.

2. Concentric ring grating concentrator

The concentric ring grating considered in this paper is illustrated in Fig. 1. It contains five concentric silver rings on top of a silver plate that contains a hole in the center. The medium surrounding the structure is taken to be free space. The geometric parameters are chosen to be: grating period p_1 = 530 nm, p_2 = 265 nm, $h_1 = h_2$ = 40 nm, d = 597.5 nm, and radius of center hole r = 200 nm. These parameters are used in all simulations of this paper.

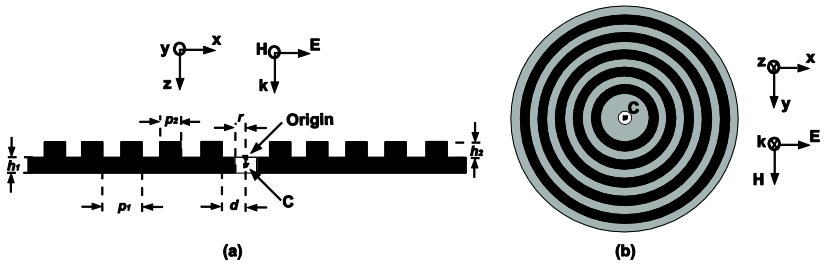

Fig. 1. (a) Cross section of a concentric ring grating concentrator. (b) Top view of the concentric ring grating concentrator. Black circles are raised Ag rings.

The concentric ring grating is designed to concentrate the incident illumination of a plane wave propagating along the + z direction, with its electric and magnetic fields polarized in the xy plane. The optical properties of silver follow a Drude model (plasma frequency is 1.163×10^{16} rad/s and collision frequency is 1.435×10^{15} rad/s) in the calculations in this paper, which have been fitted to the data in Ref [12].

#137744 - $15.00 USD Received 4 Nov 2010; revised 17 Dec 2010; accepted 25 Dec 2010; published 20 Jan 2011

As reviewed in Ref [13], the dispersion relation of the surface plasmon at the interface between metal and dielectric half-spaces is given by Eq. (1).

$$k_\rho = k_0 \sqrt{\frac{\varepsilon_d \varepsilon_m(\omega)}{\varepsilon_d + \varepsilon_m(\omega)}}. \quad (1)$$

In Eq. (1), k_0 is the wave vector in air, ε_d is the relative permittivity of the dielectric and $\varepsilon_m(\omega)$ is the dispersive relative permittivity of the metal. For the case of a plane wave normally incident on a flat air-metal boundary, the incident wave has no wavevector component parallel to the boundary, and surface plasmons are not excited. On the other hand, the inclusion of a concentric ring grating with a period of p_1 on the boundary adds a wave vector component $k_\rho = 2\pi/p_1$, enabling surface plasmon excitation. For $p_1 = 530$ nm, taking the optical properties of silver used here, Eq. (1) predicts the excitation of the surface plasmon wave for illumination at $\lambda = 570$ nm. To study the field enhancement properties, we perform a numerical simulation of the ring grating using the finite difference time domain (FDTD) method. The simulated structure is situated in free space. This is realized by using perfectly matched layers at the x, y and z boundaries. A uniform mesh size of 4 nm is chosen for the simulations of the concentric ring grating. The incident wave propagates along the + z direction, with the electric field polarized in the x direction and magnetic field polarized in the y direction. The amplitude of the x component of the electric field, normalized to the incident field, at the center of the ring grating is shown in Fig. 2(a). In the discussion that follows, the "center" of the ring grating or the antenna is point C of Fig. 1(a). This is at the midpoint, in the xy plane, of the circular rings or the antenna gap, and 20 nm from the origin (see Fig. 1(a)) in the z-direction. The amplitude peaks for a free space wavelength of $\lambda = 585$ nm, where the best concentration is achieved. This deviates slightly from the wavelength predicted by Eq. (1) ($\lambda = 570$ nm). Such a deviation is not unexpected, since the grating is placed on a silver plate of a finite thickness ($h_2 = 40$ nm). In addition to the five ring grating, we also simulate the four ring and the three ring cases. The peak values of the normalized amplitude of the x component of the electric field at the center of the four ring grating and the three ring grating are 5.53 and 4.65, respectively. Both of them are smaller than the peak value of 6.47 achieved by the five ring grating. This indicates that the propagation loss is small enough for the surface plasmon waves excited at the outer rim of the five ring grating to propagate to the center. We will consider the five ring grating in the remainder of this paper.

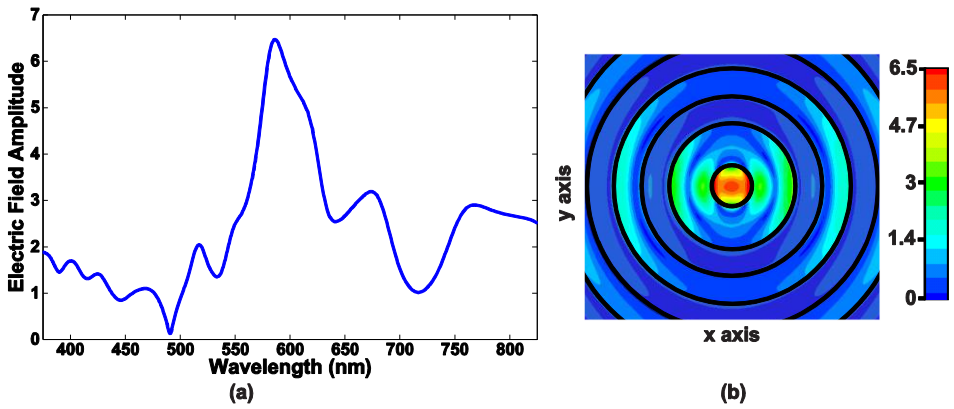

Fig. 2. (a) Normalized x component of electric field at the center of the concentric ring grating concentrator. (b) Field distribution of central portion of concentric ring grating concentrator. Plot of the amplitude of x component of normalized electric field on top surface of the grating, for excitation at $\lambda = 585$ nm.

#137744 - $15.00 USD Received 4 Nov 2010; revised 17 Dec 2010; accepted 25 Dec 2010; published 20 Jan 2011

In Fig. 2(b), the amplitude of the x component of the electric field profile on the top surface of the five ring grating is shown. The field amplitude plotted in Fig. 2(b) has been normalized to the incident field. At the center of the concentric ring grating concentrator, the y and z components of the electric field are far smaller than the x component, and are therefore not plotted. From Fig. 2(b), it can be seen that electric fields are enhanced in the hole region. The spot asymmetry follows from the incident electric field being x-polarized. Along the x-direction, the field peaks at the center and at the edges of the hole. For comparison, we conduct an FDTD simulation of the structure without the grating, i.e. a silver plate containing a hole. A field distribution similar to that of Fig. 2(b) results, but with a ~6 fold reduction in the field intensity (square of electric field), is observed for the structure without the grating.

3. Integration of an optical antenna on the concentric ring grating

As shown in Fig. 3, we now consider a fan-rod optical antenna, which will be integrated with the concentric ring grating later in this paper. Each half of the antenna consists of a rod and a flared semicircular part. The rod is intended to provide a good confinement of charges at its apex, and the flared section to act as a reservoir of charges [14]. This element combines the advantages of rod and bowtie antennas [3,5,14].

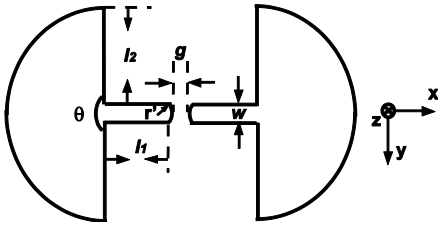

Fig. 3. Fan-rod optical antenna.

In our FDTD simulation, the following geometric parameters are chosen for a silver antenna: g = 10 nm, r' = 30 nm, w = 20 nm, l_1 = 17 nm, l_2 = 33 nm, and $\theta = \pi$. These are chosen to make the antenna resonant at λ = 585 nm, the same wavelength at which the ring grating of Section 2 achieves peak enhancement. The antenna thickness along the z direction is 40 nm. In the fan-rod antenna simulations, a non-uniform mesh is chosen, with a spacing of 2 nm for the antenna and its vicinity, and 4 nm for other regions.

As shown in the inset of Fig. 4(a), the fan-rod antenna is positioned in the center hole of the ring grating. In the simulation, the incident wave propagates along the z direction with its electric field polarized in the x direction and its magnetic field polarized in the y direction. The normalized intensities of the x component of the electric field (E_x^2) at the center of the structures are shown in Fig. 4(a), for a single antenna and for an antenna integrated with a ring grating.

#137744 - $15.00 USD Received 4 Nov 2010; revised 17 Dec 2010; accepted 25 Dec 2010; published 20 Jan 2011

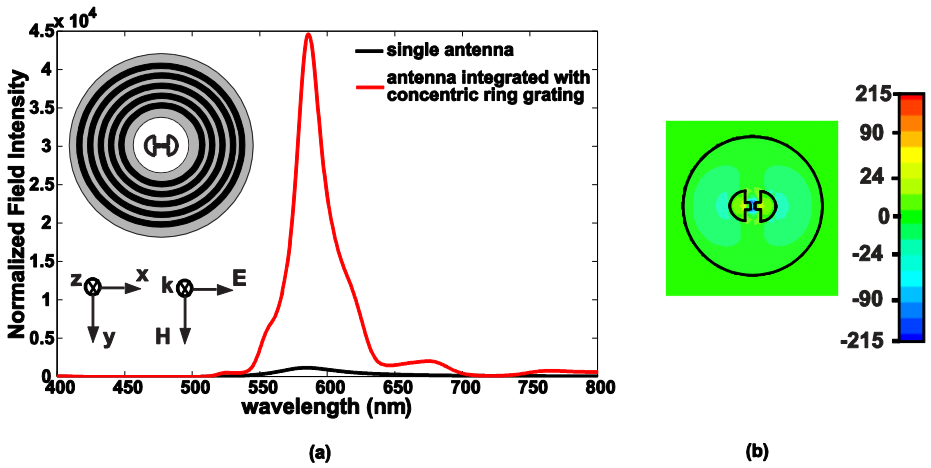

Fig. 4. (a) E_x^2 at the center of a fan-rod antenna normalized to the incident wave, for a single antenna and an antenna integrated with a concentric ring grating. Inset: schematic of simulated structure. (b) Plot of instantaneous value of x component of normalized electric field, for excitation at $\lambda = 585$ nm.

The field intensity at the center of the optical antenna is enhanced 1.19×10^3 times by a single antenna, and is enhanced 4.46×10^4 times by an antenna integrated with a ring grating, at the resonant wavelength of $\lambda = 585$ nm. This is due to the plane wave illumination being concentrated by the ring grating to its center hole, where the antenna is located. A plot of the instantaneous x component of the normalized electric field E_x on the antenna surface for illumination at $\lambda = 585$ nm is shown in Fig. 4(b). The field intensity is highly localized in the antenna gap and greatly enhanced, which is favorable for SERS.

In the above analysis, we have calculated field enhancement under plane wave illumination, an assumption employed almost universally in optical antenna analysis (e.g [2–5].), with a few exceptions [15–17]. Typically, however, an aplanatic lens, such as a microscope objective, would be used to focus light onto the antenna. An interesting question is therefore the effect of focused illumination on the field enhancement achieved both in the single, isolated antenna case, as well as the antenna integrated with the grating. This is considered in Section 5.

4. Directionality enhancement

In order to collect the Raman scattering signals efficiently it is favorable to collimate the Raman scattering into a small solid angle. In this section, we show that the Raman scattering from molecules on an antenna integrated with a concentric ring is well collimated, which improves the effective Raman scattering enhancement factor. For simplicity, we consider the molecules to be placed in the gap of the optical antenna.

A point dipole is used in our simulations to model the Raman scattering molecule. We have conducted simulations for the case of a point dipole at the center of a fan-rod antenna, and for the case of a point dipole at the center of a fan-rod antenna integrated with a concentric ring grating. The point dipole is polarized along the x direction and has the same dipole moment in both simulation cases. The far field radiation patterns in the yz plane and the xz plane are shown in Fig. 5 for a dipole whose free space wavelength is $\lambda = 585$ nm.

#137744 - $15.00 USD Received 4 Nov 2010; revised 17 Dec 2010; accepted 25 Dec 2010; published 20 Jan 2011

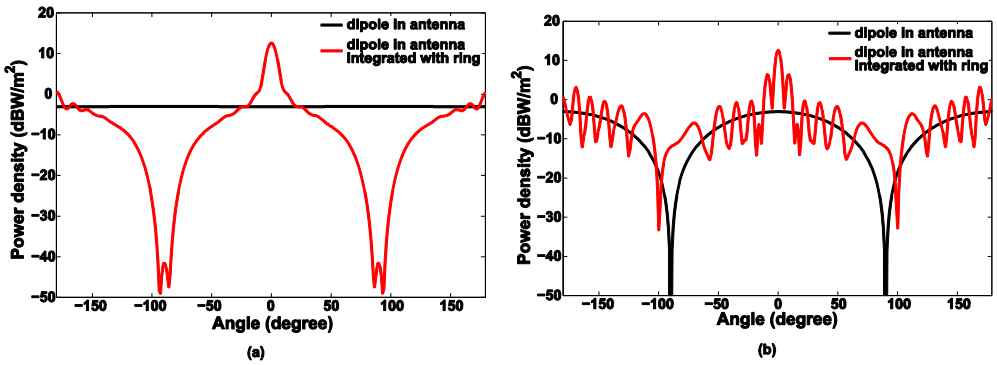

Fig. 5. Far field radiation patterns of a point dipole at the center of a fan-rod antenna, and a point dipole at the center of a fan-rod antenna integrated with a concentric ring grating. The angles in the plots are the angles between the observation directions and the -*z* direction. The unit dBW/m^2 is defined as 10 × log(power density). (a) *yz* plane. (b) *xz* plane.

Figure 5 shows that the radiation from a point dipole located at the center of the fan-rod antenna is more collimated into the -*z* direction when the antenna is integrated with a concentric ring grating. This is a reciprocal process to the ring grating's concentration of plane wave illumination into a small spot. It is interesting to notice that the radiation into the –*z* direction from the antenna-integrated-with-ring-grating structure is much stronger than into the + *z* direction. The rings function as an array of scatterers that collimate the radiation from the point dipole. The collimated radiation has a 3dB angle-width of 8.5° in the *yz* plane and 4.5° in the *xz* plane, while without the ring grating the radiation is spread into a wider range of angles. Without the ring grating, the power density varies by less than 3dB for observation points in the yz plane (Fig. 5 (a)), and a 3dB angle-width of 87° in the xz plane is predicted (Fig. 5 (b)). In order to understand the effect of the radiation pattern upon the collection efficiency achieved in an experiment, it is necessary to consider the NA of the collection lens. The collection efficiency in this paper is defined as the power collected by the objective divided by the total power radiating from the structure. The power radiated by the dipole but absorbed by metal is not included in the total radiation power for the determination of collection efficiency. If we use a microscope objective of NA = 0.7 to collect the radiation, the collection efficiency is 69.7% for a dipole located at the center of the fan-rod antenna integrated with a ring grating, while the collection efficiency is only 29.8% without the ring grating. The latter is very close to the expected collection efficiency for a point dipole radiating into free space. In Table 1, the collection efficiencies for a dipole located at the center of the fan-rod antenna integrated with and without the concentric ring grating with collection lenses of different NAs are listed. As we discuss further below, however, integration of the antenna with the ring grating increases the collected power more than the ratio of the collection efficiencies of Table 1. This is because the total radiated power is increased by the integration of the antenna with the ring grating.

Table 1. Collection efficiencies for a dipole located at the center of the fan-rod antenna integrated with and without the concentric ring grating for lenses with different NAs

NA	With grating	Without grating
0.1	46.9%	4.47%
0.4	64.5%	17.4%
0.7	69.7%	29.8%

From Table 1, it can be seen for low, medium and high NAs, collection efficiencies are improved by the concentric ring grating. Indeed, the collection efficiency with the grating structure using a low NA lens (0.1) is superior to that without the grating with a high NA lens (0.7).

#137744 - $15.00 USD Received 4 Nov 2010; revised 17 Dec 2010; accepted 25 Dec 2010; published 20 Jan 2011

A dipole with a given dipole moment can radiate more power when placed in an antenna's vicinity, a phenomenon known as the Purcell effect [18]. The power intensity radiating into the $-z$ direction, i.e. into a direction opposite to that of the illumination, is enhanced 1.19×10^3 times for the fan-rod antenna compared to the radiation from the same dipole in free space. Similarly, for a fan-rod antenna integrated with the ring grating, the enhancement is 4.37×10^4 times. These enhancement factors are in good agreement with the field intensity enhancement factors simulated found in Section 3 for the case of incident waves in the $+z$ direction. This is expected from the reciprocity theorem [19], because the dipole couples to the external optical mode with the same strength as the external optical mode excites the dipole. The total radiation power from the antenna-only structure is enhanced 1.19×10^3 times. That this is the same factor as the $-z$ direction intensity enhancement is due to its radiation pattern being very close to that of a point dipole in free space. The total radiation power from the antenna-grating structure is enhanced 2.03×10^3 times, compared to a dipole in free space. That this is smaller than its $-z$ direction intensity enhancement is due to its radiation into wider angles being weak. As noted above, the improvement that comes through the integration of the antenna with the ring is not the ratio of the collection efficiencies of Table 1. Rather, one needs to take into account the fact that the total radiation power is ~1.7 times larger for the antenna-ring structure than the antenna-only structure. In addition to predicting performance, the calculations permit us to interpret the role of the grating. The intensity at the center of the antenna under external illumination at normal incidence is ~38 times larger for the antenna-ring structure than the antenna-only structure. That this is much larger than the increase in radiation power indicates that the ring grating is more of a concentrator than a resonator.

5. Raman scattering enhancement

We now calculate the enhancement in the collected SERS signals that should result from use of the antenna-only and antenna-ring structures. We consider Raman scattering from a molecule at the center point of the structure, i.e in the antenna gap. For simplicity, we assume both the illumination and the Raman scattering are at the resonant wavelength of 585 nm, i.e. that the Stokes shift is zero. The enhancement factors we calculate are comparisons between the collected SERS signals from a molecule in the antenna-only or antenna-ring structures to those from a molecule in free space, with illumination and collection optics unchanged. A common approach for calculating SERS electromagnetic enhancement factor is to take it as the fourth power of the electric field enhancement under plane wave illumination. This assumes plane wave illumination and collection, i.e. that the NA of illumination and collection optics approach zero. Rather than using this approach, we instead calculate SERS electromagnetic enhancement factor using the following equation which accounts for the NA of illumination and collection optics:

$$EF = \left(\frac{E^2\big|_{with\ antenna}}{E^2\big|_{free\ space}}\right)\left(\frac{P_{rad}\big|_{with\ antenna}}{P_{rad}\big|_{free\ space}}\right)\left(\frac{\eta_{collection}\big|_{with\ antenna}}{\eta_{collection}\big|_{free\ space}}\right). \qquad (2)$$

The first term in parentheses is the ratio of the intensity (square of electric field) of illumination at the dipole position in an antenna-only or antenna-ring structure to the intensity of illumination at the dipole position in free space. For calculating each of these intensities, focused illumination with a given NA is employed, as described below. The second term in parentheses is the ratio of the power radiated by a dipole with a given dipole moment in an antenna-only or antenna-ring structure to that radiated when the dipole is in free space. The third term in parentheses is the ratio of the collection efficiencies at a given NA for a dipole in an antenna-only or antenna-ring structure to that for a dipole in free space.

To calculate the first term in parentheses of Eq. (2), we employ the vector diffraction theory of Richards and Wolf [20] that describes a method by which the fields at the focus of a lens illuminated by a plane wave can be found. Because we consider a dipole oriented in the x

#137744 - $15.00 USD Received 4 Nov 2010; revised 17 Dec 2010; accepted 25 Dec 2010; published 20 Jan 2011

direction, we only consider the x component of the electric field. From Ref [20], the x component of the electric field at the focus of a lens with $NA = sin\theta_{max}$ is given by:

$$E_x\big|_{free\ space} = \frac{ikfe^{-ikf}}{2\pi}\int_0^{\theta_{\max}}\int_0^{2\pi} E_\infty(\theta,\varphi)\sin\theta\ d\varphi\, d\theta,$$
$$E_\infty(\theta,\varphi) = E_0\frac{1}{2}\left[(1+\cos\theta)-(1-\cos\theta)\cos 2\varphi\right](\cos\theta)^{1/2}. \quad (3)$$

In Eq. (3), k is the wavevector in free space, f is the focal length of the objective and E_0 is the amplitude of the electric field of the plane wave.

In Eq. (3), the x component of the electric field at the focus is found by integration of the plane waves converging to the focus over possible angles of incidence. To modify this expression for the case of focused illumination incident on an antenna-only structure or antenna-ring structure, each of the plane wave components must be multiplied by a prefactor. The prefactor is equal to the electric field enhancement occurring for plane wave illumination of the antenna-only structure or antenna-ring structure at the angle of incidence. To determine the prefactor, one could perform a series of simulations of the field resulting from plane wave illumination of the antenna-only structure or antenna-ring structure at different angles of incidence. However, it is also possible to determine the prefactor from a single simulation, in which a dipole is placed at the center of the antenna-only or antenna-ring structure, and the far-field radiated at different angles is found. Because of the reciprocity theorem, this single simulation yields the required information. In Ref [19], reciprocity theorem is used to find the relationship between radiated far-fields and local fields. In Ref [19], two dipoles, and the fields that they create, are considered. A dipole $\vec{d}_0$ is placed in the vicinity of arbitrary nanostructures, and generates an electric field $\vec{E}_{far}$ at some position in the far-field. A dipole $\vec{d}_{far}$ is placed at this far-field position, and generates field $\vec{E}_{loc}$ at the position of dipole $\vec{d}_0$. These dipole moments and fields are related by:

$$\vec{d}_0 \cdot \vec{E}_{loc} = \vec{d}_{far} \cdot \vec{E}_{far}. \quad (4)$$

Following this approach, we place a dipole with dipole moment $\vec{d}_{far}$ oriented perpendicular to the radial direction $\hat{r}$ far from the antenna-only or antenna-grating structure. Because the distance from the antenna-only or antenna-grating structure to the dipole $\vec{d}_{far}$ is much greater than the wavelength, the field generated by the dipole $\vec{d}_{far}$ that illuminates the antenna-only or antenna-grating structure can be regarded as plane wave. If the orientation $\hat{e}_p(\theta,\varphi)$ of the dipole $\vec{d}_{far}$ is along the polarization direction of the field generated by the objective lens and the magnitude d_{far} of the dipole moment $\vec{d}_{far}$ is chosen appropriately, the fields generated by the dipole $\vec{d}_{far}$ that illuminate the antenna-only or antenna-grating structure are same as those that would be generated by the objective lens. Following Eq. (4), we obtain:

$$d_0\hat{x}\cdot\vec{E}\big|_{with\ antenna}(\theta,\varphi) = d_{far}\hat{e}_p(\theta,\varphi)\cdot\vec{E}\big|_{far\ with\ antenna}(\theta,\varphi), \quad (5)$$

where $d_0\hat{x}$ is the dipole moment of the dipole used to model the Raman scattering molecule, $\vec{E}\big|_{with\ antenna}(\theta,\varphi)$ is the enhanced electric field at the center of the antenna-only or antenna-grating structure, and the direction $\hat{e}_p(\theta,\varphi)$ of $\vec{d}_{far}$ is the polarization direction of the wave

#137744 - $15.00 USD Received 4 Nov 2010; revised 17 Dec 2010; accepted 25 Dec 2010; published 20 Jan 2011

generated by the objective lens as given in Ref [20]. $\vec{E}|_{far\ with\ antenna}(\theta,\varphi)$ is the far-field at the position at which the dipole $\vec{d}_{far}$ is placed, generated by the dipole $d_0\hat{x}$. Similarly, when the antenna-only or antenna-grating structure is removed, the reciprocity theorem [19] yields the following:

$$d_0\hat{x}\cdot\vec{E}|_{with\ antenna\ removed}(\theta,\varphi) = d_{far}\hat{e}_p(\theta,\varphi)\cdot\vec{E}|_{far\ free\ space}(\theta,\varphi), \tag{6}$$

where $\vec{E}|_{far\ free\ space}(\theta,\varphi)$ is the far field generated by dipole $d_0\hat{x}$ in the absence of the antenna-only or antenna-grating structure and $\vec{E}|_{with\ antenna\ removed}(\theta,\varphi)$ is the field generated by $\vec{d}_{far}$ at the place where $d_0\hat{x}$ is placed in the absence of the antenna-only or antenna-grating structure. Comparing Eqs. (5) and (6) yields the field enhancement prefactor:

$$W(\theta,\varphi) = \frac{E_x|_{with\ antenna}(\theta,\varphi)}{E_x|_{with\ antenna\ removed}(\theta,\varphi)} = \frac{\hat{e}_p(\theta,\varphi)\cdot\vec{E}|_{far\ with\ antenna}(\theta,\varphi)}{\hat{e}_p(\theta,\varphi)\cdot\vec{E}|_{far\ free\ space}(\theta,\varphi)}. \tag{7}$$

As indicated by the subscript *x*, this represents the field enhancement of the *x* component of the electric field.

Using Eqs. (5), (6) and (7), the *x* component of the electric field at the center of the antenna-only or antenna-grating structure is given by:

$$E_x|_{with\ antenna} = \frac{ikfe^{-ikf}}{2\pi}\int_0^{\theta_{\max}}\int_0^{2\pi} W(\theta,\varphi)E_\infty(\theta,\varphi)\sin\theta\, d\varphi\, d\theta. \tag{8}$$

Using Eqs. (3) and (8), the first term of Eq. (2) is found for both the antenna-only and antenna-ring structures.

The second term of Eq. (2) is $1.19\acute{}10^3$ times for the antenna-only structure, and $2.03\acute{}10^3$ times for the antenna-grating structure, as described in Section 4.

The third term of Eq. (2) is very close to unity for the antenna-only structure, as its radiation pattern is almost identical to that of a point dipole. For the antenna-grating structure, this term is equal to the ratio of collection efficiencies of the with- and without-grating structures of Table 1. The third term of Eq. (2) is therefore equal to 10.49, 3.71 and 2.34 for NAs of 0.1, 0.4 and 0.7, respectively.

Using Eqs. (2)-(8), the SERS electromagnetic enhancement factors of the antenna-grating and antenna-only structures are calculated in Table 2 for different NAs of the lens used to focus light onto, and collect light from, the device. In Table 2, we assume equal NA values of illumination and collection optics. In experiments, if the collimated excitation laser beam does not fill the whole aperture of the focusing lens, the illumination optics will have a smaller NA, and the ring grating will contribute to a larger enhancement factor than in Table 2 by its additional concentration of illumination.

Table 2. SERS electromagnetic enhancement factors of antenna-grating and antenna-only structures calculated for different NAs of illumination/collection optics

NA	Antenna-grating structure	Antenna-only structure
0.1	$2.23\acute{}10^8$	$1.35\acute{}10^6$
0.4	$1.01\acute{}10^7$	$1.35\acute{}10^6$
0.7	$4.27\acute{}10^6$	$1.35\acute{}10^6$

From Table 2, it can be seen that the antenna-grating structure is predicted to achieve higher values of SERS enhancement factors than the antenna-only structure. The improvement is particularly dramatic when the NA is low (0.1), achieving a value of ~165 times. At medium (0.4) and high (0.7) values of NA, the improvement factors are ~7.5 and

#137744 - $15.00 USD Received 4 Nov 2010; revised 17 Dec 2010; accepted 25 Dec 2010; published 20 Jan 2011

~3.2 times, respectively. That the improvement arising from the use of the grating is greatest at low NA is due to the fact that the additional focusing it provides is most advantageous when the illumination is weakly focused and the collection angle is small. It is interesting to note that the enhancement factor for the antenna-only structure is not affected by the NA. This is due to the fact that, like the molecule being modeled, the far-field radiation pattern of the antenna is almost identical to that of a point dipole. The first term in parentheses of Eq. (2) is therefore not affected by the NA. The second term does not depend on the NA. The third term is close to unity because of the fact that the radiation patterns of the dipole in free space, and the dipole in the antenna are almost identical.

As described above, the integration of the antenna with the grating improves performance by concentrating the input illumination to improve excitation, and collimating the Raman scattering to improve collection efficiency. Despite minor improvements with high NA lenses, gratings are more versatile and less expensive than high NA glass lenses. Thus far, we have considered an antenna with its dipole moment in the plane of the substrate. Another interesting possibility is discussed in the following paragraph.

The field intensity and the Purcell effect, and consequently the Raman enhancement factor of the antenna, increase significantly with shortening the gap. While a 10 nm gap is about the limit of planar lithographic techniques, such as electron beam lithography and focused ion beam modification, it is easy to achieve a distance of less than 1 nm in the vertical direction between the tip of an atomic force microscope and a planar surface. It is interesting to consider whether one could perform tip-enhanced Raman scattering (TERS) with molecules at this position [21]. In TERS experiments, it is necessary to ensure that there be an appreciate component of the electric field along the tip axis for field enhancement. A spiral ring device could offer a means for optimizing this. Using spiral rings, as distinct from the concentric rings considered in this paper thus far, an electric field polarization vertical to the substrate can be achieved at the center of the pattern [22].

6. Conclusions

We have conducted a theoretical study on the use of concentric ring gratings to improve the performance of optical antennas for SERS. Improvements to the excitation intensity, radiated power and collection efficiency were considered for different values of NA. The results revealed that the grating is predicted to improve the SERS enhancement factor by close to two orders of magnitude at low NA (0.1), close to an order of magnitude at moderate NA (0.4), and by several times at high NA (0.7). We anticipate that both the results and calculation methodology we introduce here could serve as a powerful approach toward the design of structures for improving the SERS performance of optical antennas.

Acknowledgments

D.W and K.C. acknowledge support from the Defense Advanced Research Projects Agency (grant# FA9550-08-1-0285) and the National Science Foundation (CAREER award, grant# ECCS-0747560). T.Y. acknowledges support from the Program for New Century Excellent Talents in University by the Ministry of Education of China and the Shanghai Pujiang Program under grant# 10PJ1405300.

#137744 - $15.00 USD Received 4 Nov 2010; revised 17 Dec 2010; accepted 25 Dec 2010; published 20 Jan 2011